THE JOURNAL OF BIOLOGICAL CHEMISTRY VOL. 291, NO. 21, pp. 11446–11459, May 20, 2016
© 2016 by The American Society for Biochemistry and Molecular Biology, Inc. Published in the U.S.A.

Evolution of Heat Sensors Drove Shifts in Thermosensation between *Xenopus* Species Adapted to Different Thermal Niches*

Received for publication, November 8, 2015, and in revised form, March 17, 2016 Published, JBC Papers in Press, March 28, 2016, DOI 10.1074/jbc.M115.702498

Shigeru Saito[‡§1], **Masashi Ohkita**[¶], **Claire T. Saito**[‡], **Kenji Takahashi**[¶], **Makoto Tominaga**[‡§], **and Toshio Ohta**[¶2]

From the [‡]*Division of Cell Signaling, Okazaki Institute for Integrative Bioscience, National Institute for Physiological Sciences, National Institutes of Natural Sciences, Okazaki, Aichi 444-8787, Japan, the* [§]*Department of Physiological Sciences, SOKENDAI (The Graduate University for Advanced Studies), Okazaki, Aichi 444-8787, Japan, and the* [¶]*Department of Veterinary Pharmacology, Faculty of Agriculture, Tottori University, Tottori 680-8553, Japan*

Temperature is one of the most critical environmental factors affecting survival, and thus species that inhabit different thermal niches have evolved thermal sensitivities suitable for their respective habitats. During the process of shifting thermal niches, various types of genes expressed in diverse tissues, including those of the peripheral to central nervous systems, are potentially involved in the evolutionary changes in thermosensation. To elucidate the molecular mechanisms behind the evolution of thermosensation, thermal responses were compared between two species of clawed frogs (*Xenopus laevis* and *Xenopus tropicalis*) adapted to different thermal environments. *X. laevis* was much more sensitive to heat stimulation than *X. tropicalis* at the behavioral and neural levels. The activity and sensitivity of the heat-sensing TRPA1 channel were higher in *X. laevis* compared with those of *X. tropicalis*. The thermal responses of another heat-sensing channel, TRPV1, also differed between the two *Xenopus* species. The species differences in *Xenopus* TRPV1 heat responses were largely determined by three amino acid substitutions located in the first three ankyrin repeat domains, known to be involved in the regulation of rat TRPV1 activity. In addition, *Xenopus* TRPV1 exhibited drastic species differences in sensitivity to capsaicin, contained in chili peppers, between the two *Xenopus* species. Another single amino acid substitution within *Xenopus* TRPV1 is responsible for this species difference, which likely alters the neural and behavioral responses to capsaicin. These combined subtle amino acid substitutions in peripheral thermal sensors potentially serve as a driving force for the evolution of thermal and chemical sensation.

Animals have evolved sophisticated physiological systems for sensing ambient temperatures, as fluctuations in environmental temperature significantly affect various biological processes. Species adapted to different thermal niches are likely to have acquired specific thermal sensitivities suitable for their respective habitats. Recent progress and understanding of the molecular mechanisms behind thermosensation has enabled us to elucidate the molecular basis for the evolution of thermosensation in the process of shifting thermal niches (1–3).

In vertebrates, peripheral sensory neurons such as dorsal root ganglion (DRG)[3] and trigeminal ganglion neurons relay temperature information to the central nervous system. During the initiation of signal transduction, thermal stimuli are transduced into electrical signals and a subset of ion channels that are thermally activated plays crucial roles in this process. These ion channels belong to the transient receptor potential (TRP) ion channel superfamily and are called "thermoTRP" (1–3). Animals possess several kinds of thermoTRP channels, which have distinctive temperature ranges for activation. For example, TRPV1 is activated by heat (4–7), whereas TRPM8 is activated by cold (1–3, 8).

Temperature sensitivity among orthologous thermoTRP channels has changed during the course of evolution (9). TRPA1 was first reported to be activated by cold in rodents (1–3); but was also reported to be activated by heat in several vertebrate lineages such as amphibians, reptiles, and birds (10–12) and is known as a non-temperature-sensitive channel in human and zebrafish (13, 14). These observations imply that functional changes in the peripheral thermosensors may have served as a driving force for the evolution of thermosensation. In addition to thermal perception, thermoTRP channels also serve as receptors for various chemicals such as TRPV1, which acts as a receptor for capsaicin, a substance contained in chili peppers (4, 7). Differences in the chemical sensitivity of thermoTRP channels have been well reported among orthologous channels (4–6, 10, 15, 16). Thus, they represent fascinating target molecules for the investigation of whether functional changes in sensory receptors have contributed to the evolution of sensory perception and overall species divergence in behavioral responses to specific stimuli.

* This work was supported by Grants-in-aid for Scientific Research 15H05927 (to M. T.), 16K07470 (to S. S.), and 26292150 (to T. O.) from the Ministry of Education, Culture, Sports, Science, and Technology of Japan. The authors declare that they have no conflicts of interest with the contents of this article.

The nucleotide sequence(s) reported in this paper has been submitted to the DDBJ/GenBank™/EBI Data Bank with accession number(s) LC061863, LC061864, LC061865, and LC061866.

[1] To whom correspondence may be addressed: Div. of Cell Signaling, Okazaki Inst. for Integrative Bioscience, Natl. Inst. for Physiological Sciences, Natl. Inst. of Natural Sciences, Okazaki, Aichi 444-8787, Japan. Tel.: 81-564-59-5286; Fax: 81-564-59-5285; E-mail: sshigeru@nips.ac.jp.

[2] To whom correspondence may be addressed: Dept. of Veterinary Pharmacology, Faculty of Agriculture, Tottori University, Tottori 680-8553, Japan. Tel./Fax: 81-857-31-5427; E-mail: tohta@muses.tottori-u.ac.jp.

[3] The abbreviations used are: DRG, dorsal root ganglion; TRP, transient receptor potential; TRPV1, transient receptor potential vanilloid 1; TRPA1, transient receptor potential ankyrin 1; Xla, *X. laevis*; Xtr, *X. tropicalis*.

Comparative analyses among closely related species with similar ecological and physiological traits, but that inhabit different thermal environments, are required for investigating the evolutionary processes of thermal adaptation. Two species belonging to the genus *Xenopus* (*Xenopus laevis* and *Xenopus tropicalis*) are fully aquatic anurans and morphologically similar to each other (17); however, the optimal temperature range for each of these two species is quite different. The optimal temperature range of *X. laevis* is 16–22 °C, whereas that of *X. tropicalis* is 22–28 °C (18, 19). Furthermore, *X. laevis* inhabits cooler regions compared with *X. tropicalis*, found in Africa, and thus these two *Xenopus* species have adapted to different thermal niches (17). In addition, the availability of genomic sequence data for both species makes them suitable for cloning and characterizing genes of interest (20). Previously, thermal responses of cold-activated TRPM8 were compared between *X. laevis* and *X. tropicalis*. However, there were no detectable differences in the thermal responses of TRPM8 between the two *Xenopus* species (8).

In the present study, we attempted to compare the thermal responses between *X. laevis* and *X. tropicalis* at the behavioral, sensory neuron, and temperature receptor levels. Nocifensive behaviors to heat stimulation and thermal sensitivity of sensory neurons were different between both species. Furthermore, thermal responses of both TRPA1 and TRPV1 also differed between the two *Xenopus* species. We found that three amino acid substitutions are largely responsible for the species differences in TRPV1 heat responses. We also were able to show that the sensitivity of TRPV1 to capsaicin differs between the two *Xenopus* species, and this is dictated by another single amino acid substitution. Subtle amino acid changes in thermoTRP channels altered their functional properties, and this may have contributed to the evolutionary shift in thermal and chemical sensation.

Experimental Procedures

All procedures involving the care and use of animals were approved by the committees for animal experimentation of the National Institute for Physiological Sciences and Tottori University (Japan).

Frog Samples—The *X. tropicalis* strain used for all experiments was the Yasuda strain, which was kindly provided by the National Bio-Resource Project of the Ministry of Education, Culture, Sports, Science and Technology in Japan (MEXT). *X. laevis* was purchased from Hamamatsu Seibutsu Kyozai (Hamamatsu, Japan). *X. laevis* and *X. tropicalis* (~5 cm) were housed in large plastic tanks placed in the same room, maintained at 20–25 °C, and used for behavioral experiments and the preparation of DRG neurons. Frogs were fed once every 2 days and kept on a 12-h light/dark cycle. Mature *X. laevis* females were kept at ~18 °C for oocyte collection.

Behavioral Experiments—Behavioral experiments were performed according to a previously described procedure (4). Briefly, a single frog (~5 cm) was placed into a glass bowl with a small amount of water (50 ml) and left for 20 min to habituate. Then capsaicin was added directly to the water, and jumping behaviors were counted before and after this addition. Capsaicin, purchased from Sigma, was dissolved into ethanol or dimethyl sulfoxide as a stock solution. The effect of heat stimulation on the frogs was observed similarly to that of capsaicin. In brief, after habituation, the water in the glass bowl was replaced with water heated to a specific temperature. The glass bowl containing the frog was then immediately immersed in a water bath at the same temperature, and jumping behaviors were counted.

Molecular Cloning of TRPV1 and TRPA1 Genes—Total RNA was extracted from the brain, spinal cord, and peripheral neurons excised from *X. laevis* and used as a template for reverse transcription with GeneRacer oligo(dT) primer (Invitrogen). To amplify the DNA fragment containing the full-length coding region of *X. laevis TRPV1a* (*Xla-TRPV1a*), the aforementioned reverse transcription product was used as a template for RT-PCR with the following primers: frog *X. laevis* TRPV1-F (5′-gattcaacaaaatgaagaaaat-3′) and *X. laevis* TRPV1-R (5′-gacagattcactcagccttg-3′); these were used to clone *Xla-TRPV1a* in a previous study (21). Using this PCR product as a template, nested PCR was performed with the following primers: *X. laevis* TRPV1-F-KpnI (5′-tcataaggtaccatgaagaaaatgggcagttc-3′) and *X. laevis* TRPV1-R-NotI (5′-tcataagcggccgctcactcagccttggatgtc-3′). The amplified DNA fragment derived from peripheral neurons was cloned into the pOX+ vector (for expression in *X. laevis* oocytes) with KpnI and NotI. The *TRPV1* DNA fragment was subcloned into the pVenus-NLS vector for HeLa cell expression (4).

To amplify the DNA fragment containing the full-length coding region of *X. laevis TRPV1b* (*Xla-TRPV1b*), RT-PCR was performed using the reverse transcription product mentioned above with the following primers: *X. laevis* TRPV1-F and *X. laevis* TRPV1-R2 (5′-tcactgctgggatgtctc-3′). Using this PCR product as a template, a second round of PCR was performed with the following primers: *X. laevis* TRPV1-F3 (5′-atgaagaaaatgggcagttccacc-3′) and *X. laevis* TRPV1b-R3 (5′-tcactgctgggatgtctcttcctg-3′). To attach the restriction enzyme recognition sites at both ends of the amplified DNA fragment, a third round of PCR was performed using the second PCR product as a template with the following primers: *X. laevis* TRPV1-F-KpnI and *X. laevis* TRPV1-R2-NotI (5′-taagcggccgctcactgctgggatgtctcttc-3′). Note that the same forward primers (*X. laevis* TRPV1-F and *X. laevis* TRPV1-F-KpnI) were used for cloning *Xla-TRPV1a* and *Xla-TRPV1b*, as both genes possess the same nucleotide sequences near the start codon in the genome sequence database. The amplified DNA fragment derived from peripheral neurons was cloned into the pOX+ vector with KpnI and NotI. *Xtr-TRPV1* was cloned into pOX+ and pVenus-NLS vectors in a previous study (4).

To amplify the DNA fragment containing the full-length coding region of *X. laevis TRPA1a* (*Xla-TRPA1a*), RT-PCR was performed using the reverse transcription product derived from the brain, spinal cord, and peripheral neurons with the following primers: *X. laevis* TRPA1a-F (5′-cggcccatggcttattccatc-3′) and *X. laevis* TRPA1-R (5′-gtaacatgcccacgtttggatg-3′). Using this PCR product as a template, a second round of PCR was performed with the following primers: *X. laevis* TRPA1a-F2-BamHI (5′-taaggatcccgacatgacgtgctcgatc-3′) and *X. laevis* TRPA1a-R2-NotI (5′-taagcggccgccacgtttggatgattacactgtgatg-3′). The amplified DNA fragment derived from peripheral neu-

rons was cloned into the pOX+ vector with BamHI and NotI. Similarly, for amplifying the full-length DNA fragment of *Xla-TRPA1b*, *X. laevis* TRPA1b-F (5′-aaagcgacatgacgtgctcg-3′) and *X. laevis* TRPA1b-R2-NotI (5′-taagcggccgcaatttacttcattttctgc-aacatgc-3′) primers were used for the first PCR, and then *X. laevis* TRPA1b-F2-BamHI (5′-taaggatcccgacatgacgtgctcgatc-3′) and *X. laevis* TRPA1b-R3-NotI (5′-taagcggccgcctagccatttctgg-cttttacagc-3′) primers were used for the second round of PCR. The amplified DNA fragment derived from the brain was cloned into the pOX+ vector with BamHI and NotI. The nucleotide sequences of newly cloned genes were determined for multiple clones to confirm that no PCR errors were included.

Construction of Chimeric and Mutant TRPV1 Channels—The LTL chimera, in which the central region of *Xtr-TRPV1* was introduced into the background of *Xla-TRPV1a*, was constructed ("L" and "T" refer to the portions of *Xla-TRPV1a* and *Xtr-TRPV1*, respectively). First, the pOX+ vector harboring *Xtr-TRPV1* (*Xtr-TRPV1*/pOX) was digested with AccI to excise the central portion of *Xtr-TRPV1*. Next, the pOX+ vector harboring *Xla-TRPV1a* (*Xla-TRPV1a*/pOX) was also digested with AccI to obtain the pOX vector possessing the N- and C-terminal regions of *Xla-TRPV1a* at both ends, and then the central portion of *Xtr-TRPV1* was ligated into this pOX vector to construct the LTL chimera. Similarly, to construct the LLT chimera, *Xla-TRPV1a*/pOX and *Xtr-TRPV1*/pOX were digested with KpnI and BglII, and the resulting DNA fragments were swapped by conventional cloning procedures. To construct the LTT chimera, BsrGI was used. To construct the LTLL chimera, PmeI and KpnI were used. To construct the LTLLL chimera, the TLTT chimera was first constructed with PmeI and KpnI, and then the TLTT chimera was partially digested with EcoRI. The resulting DNA fragment containing the N-terminal portion of *TRPV1* was ligated into *Xtr-TRPV1*/pOX, which was digested with EcoRI.

Xenopus TRPV1 point mutants were constructed according to the procedures described in the QuikChange site-directed mutagenesis kit (Stratagene) with minor modifications. The point mutation was introduced by PCR using the *Xla-TRPV1a*/pOX or *Xtr-TRPV1*/pOX as templates with oligonucleotide primers containing the intended mutations. The amplified PCR products were transformed into *Escherichia coli*, and then pOX+ vectors containing *TRPV1* were purified using standard procedures. The entire coding sequences of *TRPV1* were determined to confirm that only the intended mutations were introduced.

Two-electrode Voltage Clamp Method—*Xenopus* TRPV1 or TRPA1 (Xtr-TRPV1, Xla-TRPV1a, Xla-TRPV1b, Xtr-TRPA1, Xla-TRPA1a, Xla-TRPA1b, TRPV1 chimeras, and TRPV1 mutants) were heterologously expressed in *X. laevis* oocytes, and ionic currents were recorded using a previously described two-electrode voltage clamp method (15). TRPV1 complementary RNA (cRNA) was synthesized using pOX(+) vectors containing *TRPV1* with the mMESSAGE MACHINE SP6 kit (Ambion) according to the manufacturer's instructions. Fifty nl of TRPV1 cRNA (100 ng/μl) was injected into defolliculated oocytes, and ionic currents were recorded 1–4 days post-injection using an OC-725C amplifier (Warner Instruments) with a 1-kHz low-pass filter and digitized at 5 kHz using Digidata 1440 (Axon Instruments). Oocytes were voltage-clamped at −60 mV. Cinnamaldehyde (Wako) was dissolved into dimethyl sulfoxide as a stock solution and further dissolved into a ND96 bath solution and applied to oocytes by perfusion. For heat stimulation, heated ND96 was applied by perfusion. The temperature was monitored with a thermistor located just beside the oocytes using a TC-344B temperature controller (Warner Instruments). To compare the current amplitudes elicited by heat stimulation between the Xla-TRPV1a and Xla-TRPV1b (Fig. 3*C*), cRNA was injected into *X. laevis* oocytes prepared from the same preparation from a single frog, and currents were recorded side by side at 3 days post-injection in three independent preparations. Current amplitudes among wild-type and mutant *Xenopus* TRPV1 were compared by recording the currents from *X. laevis* oocytes at 3 days post-injection with two independent preparations (Figs. 7 and 8*B*). To compare the thermal activation thresholds of TRPV1 or TRPA1, currents were recorded side by side from cRNA-injected oocytes from at least three independent preparations (Figs. 3*F* and 11*G*).

Calcium Imaging in DRG Neurons and HeLa Cells—The procedures for DRG neuron preparation from frogs and subsequent calcium imaging were described previously in detail (4). Frogs (~5 cm) were sacrificed by decapitation, and the isolated DRGs were enzymatically dissociated in Liebowitz-15 (Gibco) tissue culture medium supplemented with collagenase P (2.5 mg/ml), dispase II (2 mg/ml), and DNase (0.5 mg/ml) (all from Roche Applied Science) for 30 min at 37 °C. Following enzyme digestion, individual cells were dissociated mechanically. The cell suspension was then centrifuged, and the cell pellet was resuspended in culture medium. Aliquots were plated onto glass coverslips coated with poly-L-lysine (Sigma) in a humidified atmosphere at ~25 °C. The cells were used for experiments within 1 day post-preparation. To prepare HeLa cells expressing TRPV1, the pVenus-NLS vectors containing *Xla-TRPA1a* or *Xtr-TRPV1* were transfected into HeLa cells using Lipofectamine reagent (Invitrogen). The transfected cells were incubated at 37 °C, and cells were used for calcium imaging experiments after a 24-h incubation.

Intracellular calcium concentration ($[Ca^{2+}]_i$) was measured with a fluorescent calcium indicator, fura-2, by dual excitation using a fluorescent imaging system with software-controlled illumination and acquisition (Aqua Cosmos, Hamamatsu Photonics, Hamamatsu, Japan) as described previously (4). To load fura-2, cells were incubated for 0.5–1 h at 37 °C with 10 μM fura-2 acetoxymethyl ester (Fura-2 AM, Molecular Probes) and 0.02% Cremophor EL (Sigma) in HEPES-buffered solution containing the following (mM): 103 NaCl, 6 KCl, 1.2 $MgCl_2$, 2.5 $CaCl_2$, 10 HEPES (pH 7.4) with NaOH). A coverslip with fura-2-loaded cells was placed in an experimental chamber mounted on the stage of an inverted microscope (IX71, Olympus, Tokyo, Japan) equipped with an image acquisition and analysis system. $[Ca^{2+}]_i$ was measured by exposing the cells to excitation lights at 340 or 380 nm, and the intensity of the respective fluorescent signals at 500 nm (F_{340} and F_{380}) was recorded; then their ratios (F_{340}/F_{380}) were calculated. All experiments were carried out at room temperature (22–25 °C) except for heat stimulation. For heat stimulation, heated HEPES-buffered solution was applied by perfusion.

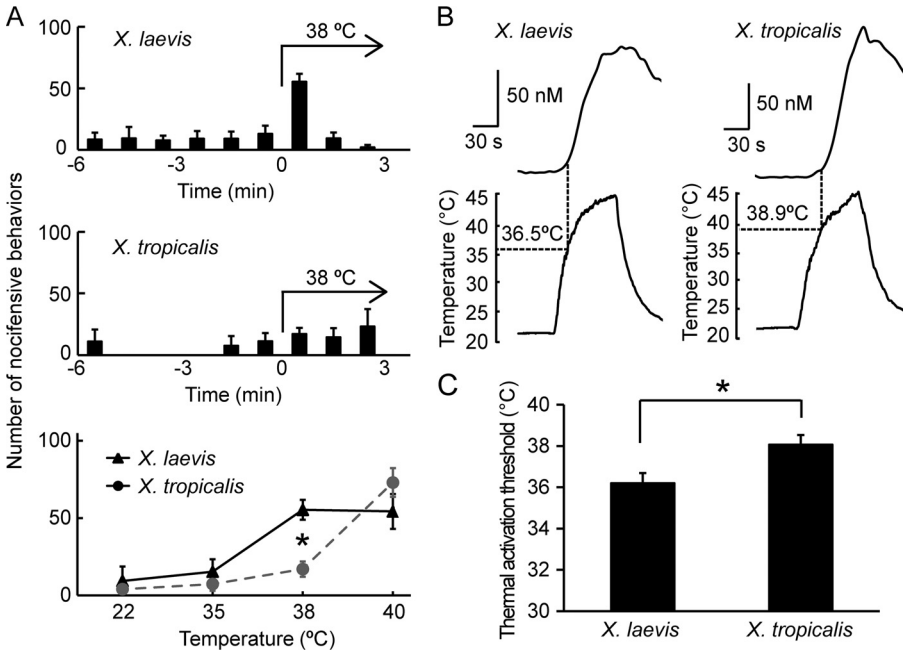

FIGURE 1. **Behavioral responses to heat and thermal sensitivity of sensory neurons differ between *X. laevis* and *X. tropicalis*.** *A*, each *bar* represents the number of jumping behaviors at 1-min intervals before and during the heat stimulations ($n = 4$ each for both *X. laevis* and *X. tropicalis*). The number of jumping behaviors in the first 1-min interval during heat stimulation is summarized (*bottom panel*, $n = 4, 5$). *, $p < 0.05$, *t* test. Note that the data for *X. tropicalis* were adopted from Ohkita *et al.* (Ref. 4, Fig. 7*F* therein). *B*, species differences in the heat response of *Xenopus* DRG neurons. Representative *traces* of $[Ca^{2+}]_i$ changes in response to heat stimulation in DRG neurons from *X. laevis* (*left*) and *X. tropicalis* (*right*). The thermal activation threshold is defined as the point at which $[Ca^{2+}]_i$ exceeds 10 nM from baseline. *C*, comparison of thermal activation thresholds of DRG neurons between the two *Xenopus* species ($n = 13$ for *X. laevis* and $n = 15$ for *X. tropicalis* from 3 frogs/species). Each data point represents the mean ± S.E. *, $p < 0.05$, *t* test.

Data Analysis—For Figs. 1, 4, and 9, part of the data for *X. tropicalis* had been obtained and published in a previous study (4). For data analysis regarding Figs. 1, 4, and 9, we obtained several new sets of data for *X. tropicalis* and reanalyzed them along with the previously obtained data. For Figs. 1*A* and 10*C*, the data for *X. tropicalis* were adopted from Ohkita *et al.* (4). All of the data, except those for Figs. 3*F* and 11*G*, are presented as the mean ± S.E. (n = number of observations). Thermal activation thresholds for *Xenopus* TRPV1 and TRPA1 were determined with an Arrhenius plot that was performed using Clampfit 10.4 and Origin 9J software. Statistical significance was tested using an unpaired *t* test for comparisons of two groups. A two-way repeated-measures analysis of variance followed by a Bonferroni multicomparison test was applied for comparing the average current amplitudes obtained by repeated heat stimulation between Xla-TRPV1a and Xla-TRPV1b groups.

For phylogenetic reconstruction, first, the amino acid sequences of TRPV1 or TRPA1 from terrestrial vertebrates were aligned by ClustalW implemented in MEGA6 (22). For estimating the evolutionary distances, all positions containing gaps were eliminated. Then the evolutionary distance (amino acid substitutions) between each pair of TRPV1 or TRPA1 sequences was estimated by JTT (Jones, Taylor, and Thornton) matrix-based methods (amino acid positions used were 691 and 1074 for TRPV1 and TRPA1, respectively) (23). Based on the estimated evolutionary distances, a phylogenetic tree was reconstructed using the neighbor-joining method (24). Bootstrap values were calculated with 1000 replications (25). All of the phylogenetic analyses were conducted using MEGA6. To examine the syntenic relationships between scaffolds containing the *TRPV1* (or *TRPA1*) paralogs of *X. laevis*, PipMaker was used to perform the dot plot analysis (26).

Results

Behavioral and Sensory Neural Responses to Heat Stimulation Differ between the Two Xenopus Species—To compare the thermal responses between *X. tropicalis* and *X. laevis*, heat stimulation was systemically applied to frogs, and nocifensive behaviors were observed. The experimental setup for observing nocifensive (jumping) behaviors was established in previous studies (4, 11). Briefly, a single frog was put into a glass bowl filled with a small amount of water. Heat stimulation was then applied by changing the water temperature, and the number of jumping behaviors was counted. Both species exhibited a similar number of jumping behaviors at 40 °C (Fig. 1*A*). However, at 38 °C, the number of jumping behaviors of *X. laevis* was significantly larger than that of *X. tropicalis*, suggesting the former species is much more sensitive to heat. Next, the response of sensory neurons to heat stimulation was compared. Primary cultured DRG neurons were prepared from both species, and changes in the intracellular Ca^{2+} concentrations ($[Ca^{2+}]_i$) were measured upon heat stimulation in Ca^{2+} imaging experiments. The level of $[Ca^{2+}]_i$ in DRG neurons from both species increased upon heat stimulation (Fig. 1*B*). The thermal activation threshold for *X. laevis* DRG neurons was significantly lower than that for *X. tropicalis* (*X. laevis*, 36.2 ± 0.5 °C, $n = 13$; *X. tropicalis*, 38.1 ± 0.4 °C, $n = 15$ (Fig. 1*C*)). We reported previously that TRPV1 and TRPA1 from *X. tropicalis* are activated by heat stimulation and are highly co-expressed in most of the heat-sensitive DRG neurons (~85%) (11). Therefore, the differences observed

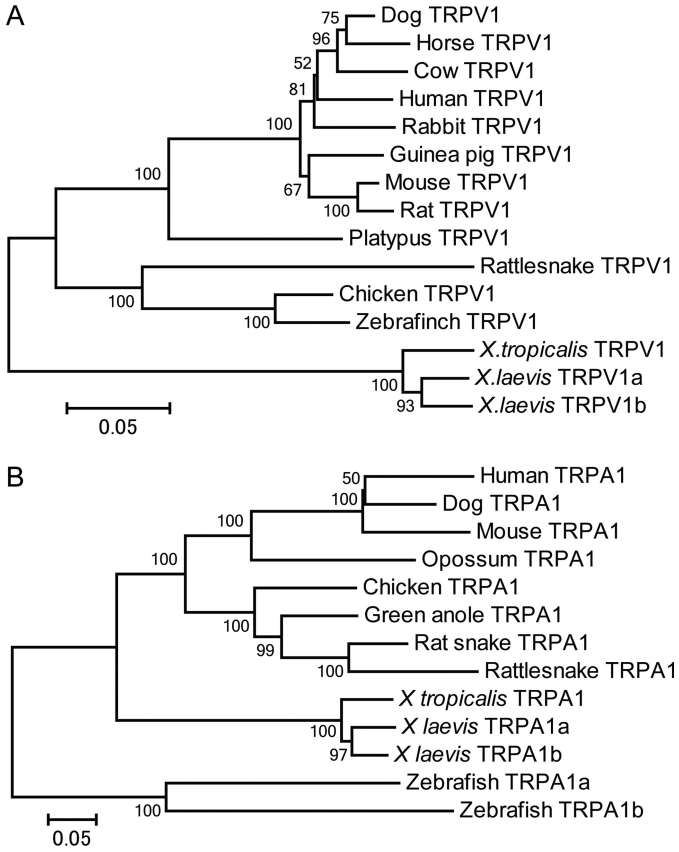

FIGURE 2. **Phylogenetic relationship of vertebrate *TRPV1* (*A*) and *TRPA1* (*B*) including *Xenopus* species.** Evolutionary distances were estimated by comparing amino acid sequences, and phylogenetic trees were reconstructed with the neighbor-joining method (24). Statistical confidence (bootstrap value) is shown beside each node of the phylogenetic tree. *Scale bar* indicates 0.05% amino acid substitutions/site.

between the two *Xenopus* species are potentially related to the functional differences in TRPV1 and/or TRPA1.

Comparison of TRPV1 Channel Properties between the Two Xenopus species—To address the possibility described above, the channel properties of TRPV1 were compared between the two *Xenopus* species. The *TRPV1* gene from *X. tropicalis* (*Xtr-TRPV1*) was cloned and characterized in our previous study (4). Therefore, we attempted to clone the *TRPV1* gene from *X. laevis*. *TRPV1* was searched in the recently released genome sequence database, and two copies were found (named *Xla-TRPV1a* and *Xla-TRPV1b*). *Xla-TRPV1a* corresponds to the *TRPV1* cloned in a previous study by another research group, although the channel properties for heat stimulation had yet to be analyzed (21). Phylogenetic reconstruction of terrestrial *TRPV1* orthologs revealed that *Xtr-TRPV1* diverged earlier than did *Xla-TRPV1a* and *Xla-TRPV1b* (Fig. 2*A*). Two copies of the *Xla-TRPV1* genes were located within different scaffolds in the genome sequence database, and syntenic relationships were conserved around *TRPV1* (data not shown). These observations suggested that the two copies of *TRPV1* were produced by a genome duplication event (allopolyploidy), which occurred in the ancestral *Xenopus* lineage after the split from the lineages leading to *X. tropicalis*. RT-PCR was performed with cDNA derived from the brain, spinal cord, and peripheral neurons, and DNA fragments containing the full-length coding regions of both *Xla-TRPV1a* and *Xla-TRPV1b* were successfully obtained from all three tissues examined.

The ion channel properties of TRPV1 were characterized by expressing the channels in *X. laevis* oocytes (hereafter simply referred to as *Xenopus* oocytes), and ionic currents elicited by heat stimulation were examined. We first compared the channel properties between Xla-TRPV1a and Xla-TRPV1b. Heat stimulation elicited inward currents in *Xenopus* oocytes expressing either channel (Fig. 3, *A* and *B*). However, heat-evoked currents in *Xenopus* oocytes expressing Xla-TRPV1a were significantly larger than those in *Xenopus* oocytes expressing Xla-TRPV1b (Fig. 3*C*); therefore, Xla-TRPV1a may play a major role in response to heat. The maximal responses of *Xenopus* oocytes expressing Xla-TRPV1a were elicited from the first heat stimulation, and the responses subsequently became smaller with repeated heat stimuli, thus exhibiting desensitization properties to heat stimulation (Fig. 3*A*). In contrast, the first heat stimulation evoked only a partial response in Xtr-TRPV1, and the current amplitudes gradually increased with repeated heat stimulation (sensitization, Fig. 3*D*). Apparent species differences in TRPV1 heat responses could be observed when current amplitudes obtained from repeated heat stimulation were normalized to the maximum current amplitudes (Fig. 3*E*).

Thermal activation thresholds for TRPV1 were calculated with Arrhenius plots using data obtained from the first heat stimulation and were compared between the two *Xenopus* species. The average temperature threshold for activation was similar between Xla-TRPV1a (40.5 ± 0.4 °C, $n = 31$) and Xtr-TRPV1 (40.8 ± 0.4 °C, $n = 18$) (Fig. 3*F*). The average thermal activation threshold values for Xtr-TRPV1 were slightly higher than the values we reported previously (4). Because the average thermal activation thresholds varied among different preparations of *Xenopus* oocytes, in the present study we compared the thermal activation thresholds between Xtr-TRPV1 and Xla-TRPV1a side by side for eight independent preparations. However, we could not detect any species difference between Xtr-TRPV1 and Xla-TRPV1a. We also compared the properties of Xla-TRPV1a and Xtr-TRPV1 by expressing them in HeLa cells and measuring $[Ca^{2+}]_i$ in Ca^{2+} imaging experiments. The level of $[Ca^{2+}]_i$ in HeLa cells expressing Xla-TRPV1a was significantly higher than that in HeLa cells expressing Xtr-TRPV1 at 38 °C (Fig. 4). In summary, the responses of TRPV1 to repeated heat stimulation were clearly different between the two *Xenopus* species (Fig. 3).

Identification of Amino Acid Substitutions Responsible for Species Differences in Xenopus TRPV1 Heat Response—Next, we sought to identify the amino acids responsible for the observed species differences in *Xenopus* TRPV1 in order to understand the molecular basis for the evolutionary changes in channel properties. The amino acid difference between Xla-TRPV1a and Xtr-TRPV1 is 7.6% (64 amino acid substitutions were observed throughout the channels). To narrow down the region responsible for the species differences, various combinations of *Xenopus* TRPV1 chimeras were constructed, and their heat responses were examined (Fig. 5*A*). When the central portion of Xtr-TRPV1 (T) was introduced onto the Xla-TRPV1a (L) background (we named it the LTL chimera), the chimera

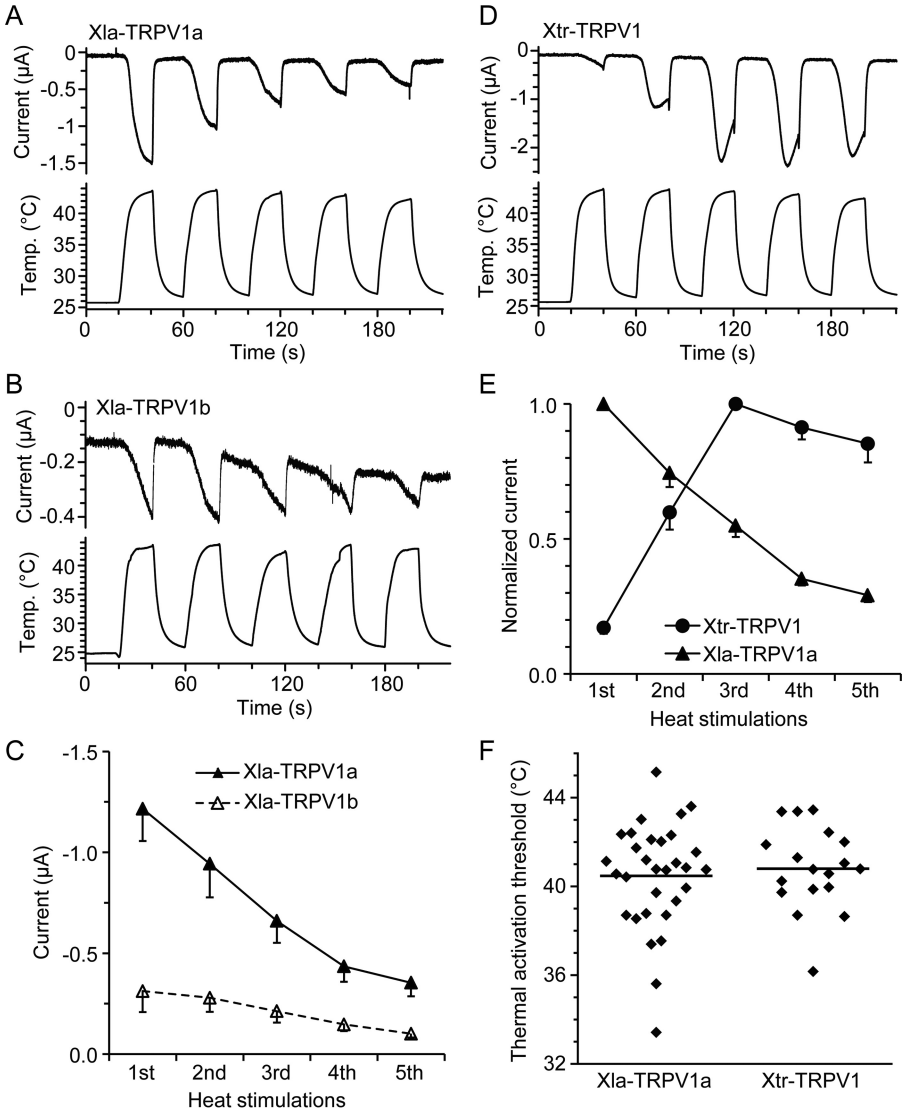

FIGURE 3. **Species differences in heat response of TRPV1 between the two *Xenopus* species.** *A*, *B*, and *D*, representative *traces* for current and temperature in *Xenopus* oocytes expressing Xla-TRPV1a (*A*), Xla-TRPV1b (*B*), and Xtr-TRPV1 (*D*) in response to repeated heat stimulation. *C*, average current amplitudes elicited by *Xenopus* oocytes expressing Xla-TRPV1a ($n = 11$) or Xla-TRPV1b ($n = 12$). For each channel, the same amount of cRNA was injected into the *Xenopus* oocytes, and current measurements were performed 3 days post-injection with three independent preparations. Current amplitudes for Xla-TRPV1a were significantly larger than those for Xla-TRPV1b (two-way repeated measures analysis of variance, $p < 0.01$). *E*, current amplitudes elicited by repeated heat stimulations were normalized to the maximum currents (the first and third heat stimulation for Xla-TRPV1a and Xtr-TRPV1, respectively) obtained from *Xenopus* oocytes expressing Xla-TRPV1a ($n = 15$) or Xtr-TRPV1 ($n = 14$) with three independent preparations. *F*, thermal activation thresholds for Xla-TRPV1a and Xtr-TRPV1. *Dots* indicate individual values obtained from different *Xenopus* oocytes (eight independent preparations) expressing Xla-TRPV1a ($n = 31$) or Xtr-TRPV1 ($n = 18$). Average values are shown by *bars*.

showed desensitization properties similar to Xla-TRPV1a (Fig. 5, *A* and *B*). Introducing the C-terminal region of Xtr-TRPV1 onto the Xla-TRPV1a background (LLT) had no effect on desensitization properties (Fig. 5*B*). In contrast, replacing the N-terminal region of Xtr-TRPV1 with that of Xla-TRPV1a (LTT) altered the channel exhibiting a maximum response during the first heat stimulation (Fig. 5*C*), suggesting that the N-terminal region is responsible for the species differences. When we constructed chimeras with shorter regions of Xla-TRPV1a on the Xtr-TRPV1 background (TLTT and TLTTT), the region responsible for the species difference was determined to be within the first three ankyrin repeat domains (domains 1–3). This region was capable of shifting the Xtr-TRPV1 channel properties to be similar to those of Xla-TRPV1a (sensitization to desensitization (Fig. 5*C*)).

Within ankyrin repeat domains 1–3, eight amino acid substitutions exist between Xla-TRPV1a and Xtr-TRPV1. Among these, amino acids are exchanged between residues having relatively different properties in three amino acid positions clustered together (positions 181, 185, and 188 in Xtr-TRPV1 (Fig. 6*A*)). Thus, we assessed the effect of these three substitutions by introducing point mutations into Xtr-TRPV1 and examining the responses of mutant channels to heat stimulation. Introducing a single mutation at position 181 or 185 (Xtr-TRPV1 N181K or Xtr-TRPV1 S185H) had little effect on the sensitization properties (Fig. 6, *B* and *C*, *left panels*), whereas a mutation at position 188 (Xtr-TRPV1 P188L) increased the responses to the first heat stimulation (Fig. 6*C*, *right panel*). This mutant channel exhibited close to the maximal response during the first heat stimulation, and repeated heat stimulation elicited

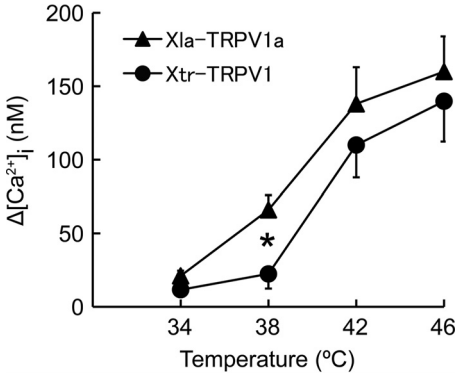

FIGURE 4. **Comparison of Xla-TRPV1a and Xtr-TRPV1 heat responses by expression in HeLa cells.** Average increase in $[Ca^{2+}]_i$ in response to heat stimulation in HeLa cells expressing Xla-TRPV1a ($n = 10–16$) or Xtr-TRPV1 ($n = 9–15$). A single heat stimulation was applied for each respective thermal stimulation. Each data point represents the mean ± S.E. *, *t* test, $p < 0.05$.

similar levels of activation (Fig. 6*B*). As Xtr-TRPV1 P188L did not show the clear desensitization properties observed in Xla-TRPV1a, we assessed the combinatory effects of mutations by constructing double and triple mutants (Xtr-TRPV1 S185H/P188L and Xtr-TRPV1 N181K/S185H/P188L). However, the channel properties of both mutants were similar to those of Xtr-TRPV1 P188L (Fig. 6*B*). Additionally, all of the Xtr-TRPV1 mutant channels possessing P188L mutations (Xtr-TRPV1 P188L, Xtr-TRPV1 S185H/P188L, and Xtr-TRPV1 N181K/S185H/P188L) had a tendency to evoke larger current amplitudes compared with those of the wild-type channel (Fig. 7*A*). In contrast, the current amplitudes elicited by capsaicin stimulation, which was applied after heat stimulation, were not statistically different between Xtr-TRPV1 P188L (−2.51 ± 0.79 μA, $n = 7$) and Xtr-TRPV1 (−3.82 ± 0.79 μA, $n = 5$) (measurements were performed 3 days post-injection), suggesting that the mutation at position 188 in Xtr-TRPV1 specifically increased the heat activity of the mutant.

The effects of the mutations at the three positions described above in TRPV1 were further examined in the reverse direction. When the point mutations were introduced into Xla-TRPV1a at position 186 (corresponding to position 188 of Xtr-TRPV1), the current amplitudes to heat stimulation became smaller compared with those of the wild-type channel (Fig. 7*B*). These observations suggested that the substitution between leucine and proline was not sufficient to explain all of the species differences in the heat response of *Xenopus* TRPV1. It is worth noting that Xla-TRPV1a K179N also showed reduced current amplitudes, although the reverse mutation in the corresponding position of Xtr-TRPV1 (N181K) had almost no effect (Figs. 6*B* and 7). This may indicate that the substitution from lysine to asparagine at this position had a minor effect on species differences in the heat response of *Xenopus* TRPV1.

Mutational analysis thus far has identified a single amino acid, which partly explains the species differences, although this mutation alone could not account for all of the species differences such as the desensitization and activity. Therefore, we sought to identify other amino acids within this region delineated by chimeric analysis (Fig. 6*A*). We selected positions at which amino acids are shared between Xla-TRPV1a and Xla-TRPV1b, although different in Xtr-TRPV1, because the former

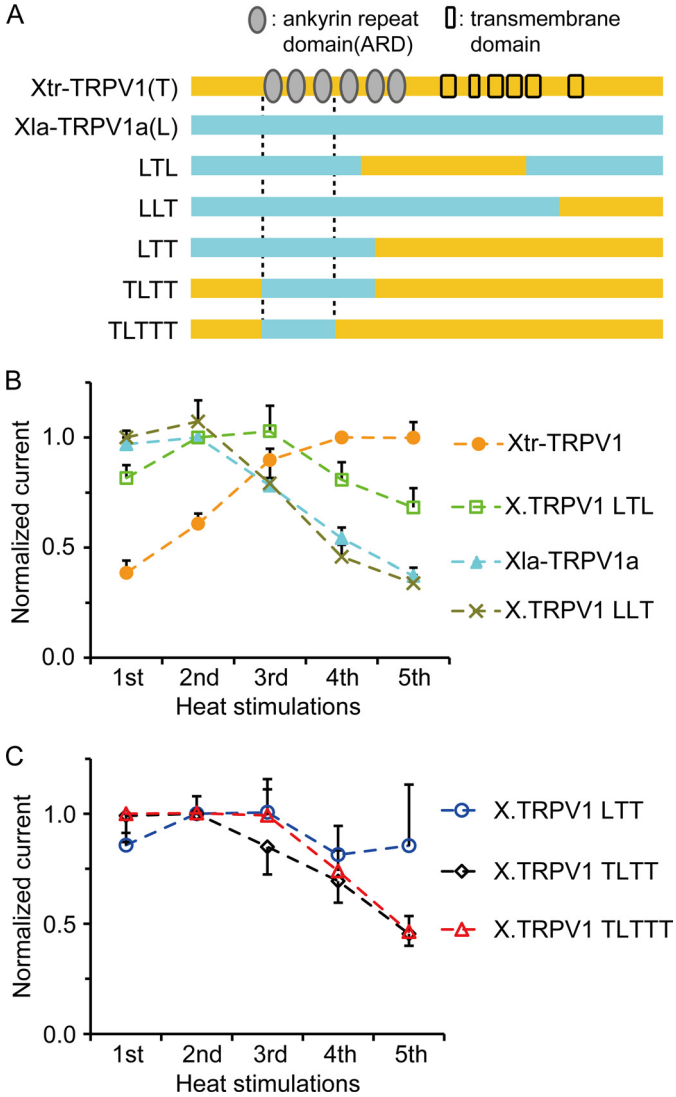

FIGURE 5. **Ankyrin repeat domains (*ARD*) 1–3 in *Xenopus* TRPV1 are responsible for the species differences in heat response.** *A*, schematic structures of the chimeras between the Xla-TRPV1a and Xtr-TRPV1 channels. The *orange* and *blue bars* represent the fragments of Xtr-TRPV1 (*T*) and Xla-TRPV1a (*L*), respectively. The names of the chimeras represent the combination of the fragments derived from the respective species. For example, in the X.TRPV1 LTL chimera, the central region of Xtr-TRPV1 was introduced onto the Xla-TRPV1a background. *B* and *C*, averaged normalized currents obtained from repeated heat stimulation in *Xenopus* oocytes expressing Xla-TRPV1a, Xtr-TRPV1, and various X.TRPV1 chimeras ($n = 16$ or 18 for Xtr-TRPV1, $n = 12$ or 14 for X.TRPV1 LTL, $n = 15$ for Xla-TRPV1a, $n = 11$ or 12 for X.TRPV1 LLT, $n = 9$ or 11 for X.TRPV1 LTT, $n = 16$ or 17 for X.TRPV1 TLTT, and $n = 9$ or 10 for X.TRPV1 TLTTT). For each of the channels, the average current amplitudes were calculated for the respective heat stimulation, and the current amplitude with the largest average value was used for normalization.

two channels exhibit properties of desensitization to repeated heat stimulation (Fig. 3, *A–C*). Four positions satisfied the criterion (positions 141, 156, 180, and 232 in Xtr-TRPV1). Single point mutants for each position were constructed. Among the four mutants, two of them (Xtr-TRPV1 K156R and Xtr-TRPV1 E232Q) showed a relatively larger heat response in the first heat stimulation compared with the wild type (Fig. 8*A*). Furthermore, the double mutant Xtr-TRPV1 K156R/E232Q exhibited close to the maximal response in the first heat stimulation (Fig. 8*A*). Notably, these three mutants (single mutants at either position 156 or 232 and double mutants at both positions)

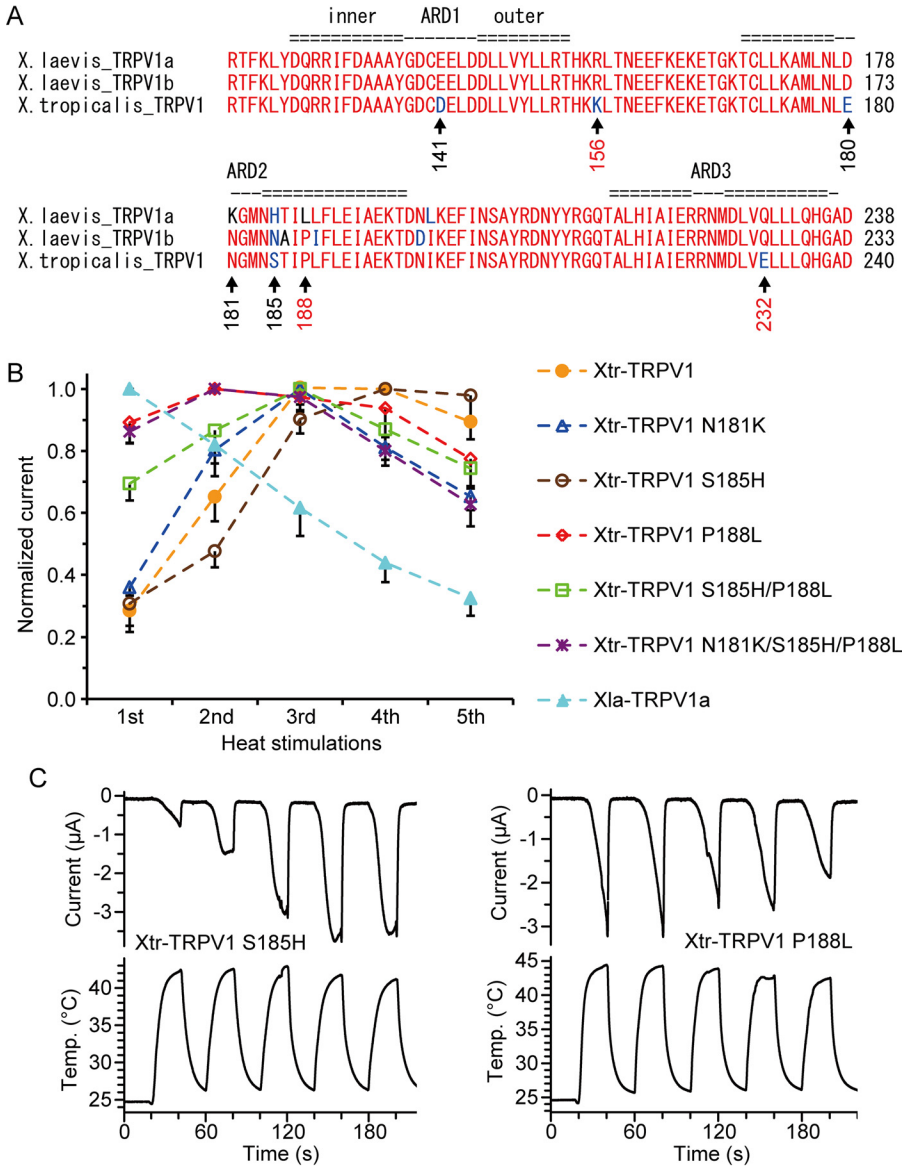

FIGURE 6. **A single amino acid substitution is involved in the species differences in TRPV1 heat responses in *Xenopus*.** *A*, amino acid sequence alignment of *Xenopus* TRPV1 within the region that was identified by the chimeric analysis shown in Fig. 5. Conserved residues are shown in *red*, and the residues substituted for similar or different amino acids are shown in *blue* or *black*, respectively. The positions where mutations were introduced are marked with *arrows*. The positions involved in the species differences in TRPV1 heat responses are shown in *red*. The *numbering* of the positions is in accordance with Xtr-TRPV1. The positions of the ankyrin repeat domains were based on rat TRPV1 (38). *B*, normalized currents elicited by *Xenopus* oocytes expressing Xtr-TRPV1 mutants (n = 10 for Xtr-TRPV1, n = 13 for Xtr-TRPV1 N181K, n = 9 for Xtr-TRPV1 S185H, n = 12 for Xtr-TRPV1 P188L, n = 12 for Xtr-TRPV1 S185H/P188L, n = 12 or 13 for Xtr-TRPV1 N181K/S185H/P188L, and n = 9 for Xla-TRPV1a). The currents were normalized to the maximum average current among five heat stimulations for each channel (the first for Xla-TRPV1a, the second for Xtr-TRPV1 P188L and Xtr-TRPV1 N181K/S185H/P188L, the third for Xtr-TRPV1 N181K and Xtr-TRPV1 S185H/P188L, and the fourth for Xtr-TRPV1 and Xtr-TRPV1 S185H) *C*, representative *traces* for current and temperature in response to repeated heat stimulation in *Xenopus* oocytes expressing Xtr-TRPV1 S185H (*left*) and Xtr-TRPV1 P188L (*right*).

showed similar current amplitudes to the wild type, suggesting that mutations at positions 156 and 232 did not alter heat activity (Fig. 8*B*). However, these mutants did not exhibit desensitization properties like Xla-TRPV1a (Fig. 8*A*). Therefore, combinatory effects with P188L mutations were further investigated by assessing Xtr-TRPV1 D141E/P188L, Xtr-TRPV1 K156R/P188L, Xtr-TRPV1 E180D/P188L, and Xtr-TRPV1 E232Q/P188L. All of these mutants possessed properties similar to those of Xtr-TRPV1 P188L (Figs. 6*B* and 8*C*). That is, they exhibited close to the maximal response from the first heat stimulation; however, they did not show clear desensitization to repeated heat stimulation. Additionally, the current amplitudes were much larger than those observed for the wild-type TRPV1 (data not shown). In summary, chimeric and mutagenesis analyses identified three amino acid substitutions (at positions 156, 188, and 232 in Xtr-TRPV1) involved in the species differences in TRPV1 heat responses between *X. laevis* and *X. tropicalis*.

A Single Amino Acid Substitution within TRPV1 Likely Dictates the Difference in Behavioral Responses to Capsaicin between the Two Xenopus Species—We reported previously that the sensitivity of *X. tropicalis* TRPV1 to capsaicin is considerably lower than that of rodent and human TRPV1, and a single amino acid substitution in the third transmembrane domain is responsible for the species differences (between ser-

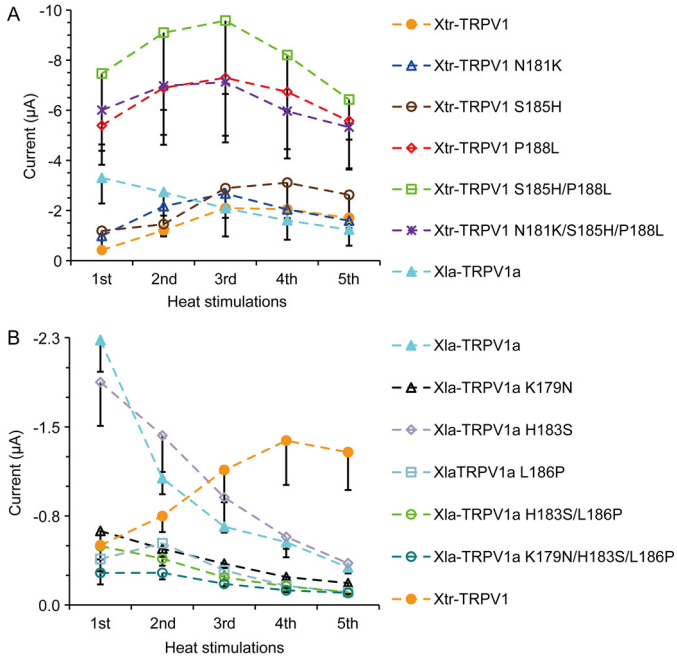

FIGURE 7. **Heat-induced activity differs among *Xenopus* TRPV1 mutants.** Average current amplitudes elicited by repeated heat stimulation in *Xenopus* oocytes expressing *Xenopus* TRPV1 mutants. *A*, $n = 7$ for Xtr-TRPV1, $n = 9$ for Xtr-TRPV1 N181K, $n = 6$ for Xtr-TRPV1 S185H, $n = 9$ for Xtr-TRPV1 P188L, $n = 8$ for Xtr-TRPV1 S185H/P188L, $n = 9$ or 10 for Xtr-TRPV1 N181K/S185H/P188L, and $n = 5$ for Xla-TRPV1a. *B*, $n = 5$ for Xla-TRPV1a, $n = 10$ for Xla-TRPV1a K179N, $n = 7$ for Xla-TRPV1a H183S, $n = 7$ for Xla-TRPV1a L186P, $n = 8$ for Xla-TRPV1a H183S/L186P, $n = 8$ for Xla-TRPV1a K179N/H183S/L186P, and $n = 7$ for Xtr-TRPV1. For each of the channels, the same amount of cRNA was injected into the *Xenopus* oocytes, and current measurements were performed 3 days post-injection.

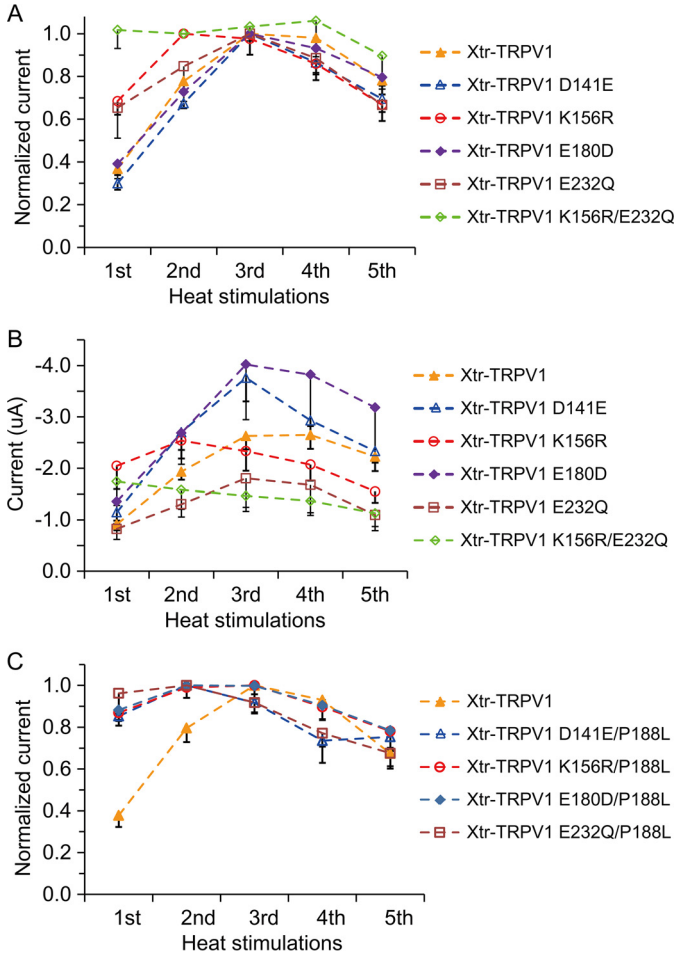

FIGURE 8. **Two conservative amino acid substitutions are also involved in species differences in the TRPV1 heat response in *Xenopus*.** *A*, normalized currents elicited by repeated heat stimulation in *Xenopus* oocytes expressing Xtr-TRPV1 mutants ($n = 16$ or 19 for Xtr-TRPV1, $n = 12$ or 13 for Xtr-TRPV1 D141E, $n = 14$ for Xtr-TRPV1 K156R, $n = 12$ for Xtr-TRPV1 E180D, $n = 12$ or 14 for Xtr-TRPV1 E232Q, and $n = 14$ or 15 for Xtr-TRPV1 K156R/E232Q). The currents were normalized to the maximum average current among five heat stimulations for each channel (the second for Xtr-TRPV1 K156R and Xtr-TRPV1 K156R/E232Q and the third for Xtr-TRPV1, Xtr-TRPV1 D141E, Xtr-TRPV1 E180D, and Xtr-TRPV1 E232Q) *B*, average current amplitudes elicited by repeated heat stimulation in *Xenopus* oocytes expressing Xtr-TRPV1 mutants ($n = 11$ or 14 for Xtr-TRPV1, $n = 7$ or 8 for Xtr-TRPV1 D141E, $n = 9$ for Xtr-TRPV1 K156R, $n = 7$ for Xtr-TRPV1 E180D, $n = 8$ for Xtr-TRPV1 E232Q, and $n = 9$ or 10 for Xtr-TRPV1 K156R/E232Q). For each of the channels, the same amount of cRNA was injected into the *Xenopus* oocytes, and current measurements were performed 3 days post-injection. *C*, normalized currents elicited by repeated heat stimulation in *Xenopus* oocytes expressing Xtr-TRPV1 mutants ($n = 5$ or 7 for Xtr-TRPV1, $n = 4$ for Xtr-TRPV1 D141E/P188L, $n = 4$ for Xtr-TRPV1 K156R/P188L, $n = 4$ for Xtr-TRPV1 E180D/P188L, and $n = 4$ or 5 for Xtr-TRPV1 E232Q/P188L). The currents were normalized to the second stimulation, except for Xtr-TRPV1 in which currents were normalized to the third stimulation.

ine and tyrosine (Fig. 9*A*)) (4). When the amino acid residues are compared at this position, Xla-TRPV1b possesses a serine, whereas Xla-TRPV1a possesses a cysteine. To assess the effect of a cysteine residue at this position, the sensitivity of Xla-TRPV1a to capsaicin was examined. HeLa cells expressing Xla-TRPV1a exhibited clear responses to lower concentrations of capsaicin compared with those expressing Xtr-TRPV1 (Fig. 9, *B* and *C*). When the cysteine at position 521 of Xla-TRPV1a was replaced with tyrosine (the same amino acid as in Xtr-TRPV1, Xla-TRPV1a C521Y), the sensitivity of the mutant channel to capsaicin became ~100 times lower than that of the wild-type channel and was comparable to that of Xtr-TRPV1 (Fig. 9, *B–E*). These observations indicated that a single amino acid substitution occurred in TRPV1 between the two *Xenopus* species that drastically shifted their sensitivity to capsaicin.

We next compared the sensitivity of primary cultured DRG neurons to capsaicin between the two *Xenopus* species. As expected, primary cultured DRG neurons from *X. laevis* responded to lower concentrations of capsaicin compared with those from *X. tropicalis* (Fig. 10*A*). All of the capsaicin-sensitive DRG neurons also responded to high concentrations of K^+, which was used to confirm the viability of the DRG neurons. The threshold concentration for *X. laevis* DRG neurons is around 0.3 μM, which is almost the same as that for HeLa cells expressing Xla-TRPV1a. The sensitivity of *X. laevis* DRG neurons to capsaicin was considerably higher than that of *X. tropicalis* neurons (Fig. 10*B*). We further compared the nocifensive behaviors against capsaicin stimulation. The number of jumping behaviors for *X. laevis* was drastically increased immediately after the addition of 10 μM capsaicin and was substantially decreased at 1 min after the addition (Fig. 10*C*, *top panel*). In contrast, the number of jumping behaviors for *X. tropicalis* increased only slightly upon exposure to 10 μM capsaicin (Fig. 10*C*, *middle panel*). Again, *X. laevis* sensitivity to capsaicin was considerably higher than that of *X. tropicalis* (Fig. 10*C*, *bottom panel*). In summary, sensitivity to capsaicin was considerably higher in *X. laevis* compared with *X. tropicalis* at the receptor, neuron, and behavioral levels (Figs. 9 and 10).

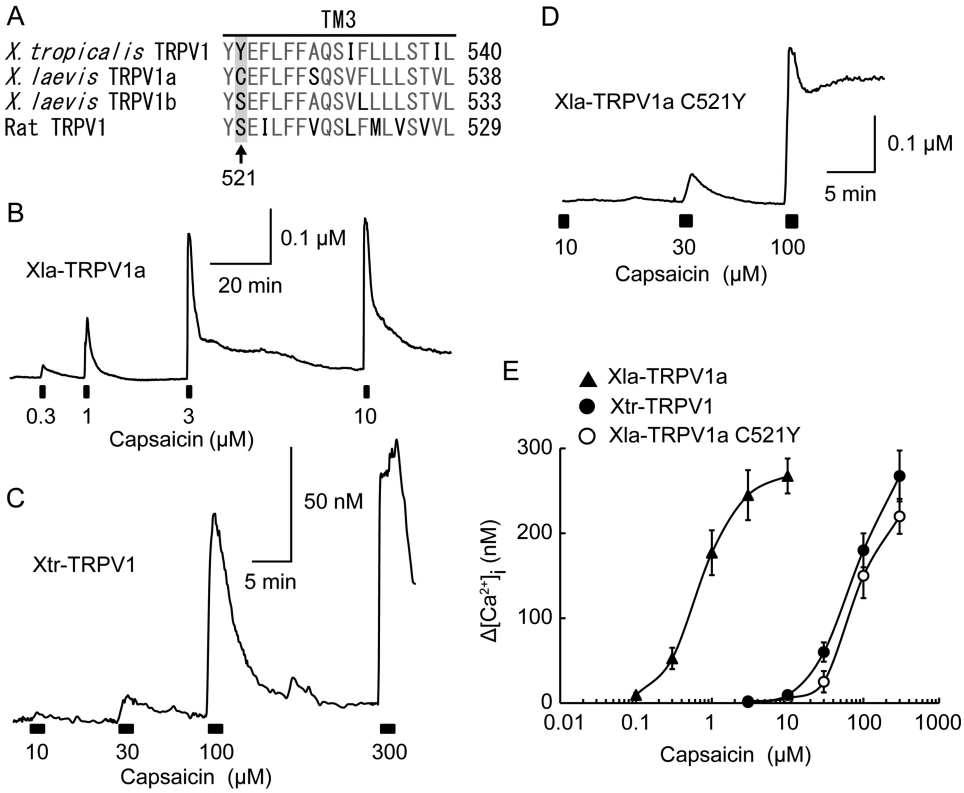

FIGURE 9. **A single amino acid substitution drastically shifted TRPV1 sensitivity to capsaicin between the two *Xenopus* species.** *A*, alignment of amino acid sequences in transmembrane domain 3 of TRPV1. The *arrow* marks the amino acid known to be involved in TRPV1 sensitivity to capsaicin. The *numbering* is based on that of Xla-TRPV1a. *B–D*, representative *traces* of dose-dependent changes in $[Ca^{2+}]_i$ in HeLa cells expressing Xla-TRPV1a (*B*), Xtr-TRPV1 (*C*), and Xla-TRPV1a C521Y (*D*) mutants in response to capsaicin stimulation with various concentrations. *E*, dose dependence of each channel in response to capsaicin ($n = 12–21$ for Xla-TRPV1a, $n = 9–13$ for Xtr-TRPV1, and $n = 10–12$ for Xla-TRPV1 C521Y).

Heat Responses of TRPA1 Differ between the Two Xenopus Species—Next, we compared the thermal responses of TRPA1 between the two *Xenopus* species. First, the *TRPA1* genes were searched in the genome sequence database of *X. laevis*, and as expected, two copies of *TRPA1* were found. Similar to *TRPV1*, a syntenic relationship was observed between the scaffolds containing *TRPA1* (data not shown), and their phylogenetic relationship (Fig. 2*B*) indicates that these two copies of *TRPA1* were produced by a genome duplication event. The full-length coding sequence of *Xla-TRPA1a* was amplified from cDNA obtained from the brain, spinal cord, and peripheral neurons, whereas that of *Xla-TRPA1b* was amplified from the brain only. *Xenopus* oocytes expressing either Xla-TRPA1a or Xla-TRPA1b elicited clear inward currents in response to heat and cinnamaldehyde stimulation (Fig. 11, *A* and *B*). The heat-induced currents showed clear desensitization during the first stimulation. To compare the thermal activation thresholds between Xla-TRPA1a and Xla-TRPA1b, heat-induced currents were recorded side by side for three independent preparations. The average thermal threshold was similar between TRPA1a and TRPA1b (Xla-TRPA1a, 36.9 ± 0.7 °C, $n = 17$; Xla-TRPA1b, 36.3 ± 0.7 °C, $n = 22$). In contrast, Xla-TRPA1a was found in all three neural tissues including peripheral neurons, whereas Xla-TRPA1b was found only in the brain, suggesting that Xla-TRPA1a may play a major role in thermal perception. Thus, heat responses between Xla-TRPA1a and Xtr-TRPA1 were compared (Fig. 11, *C* and *F*). The thermal activation threshold of Xla-TRPA1a was significantly lower than that of Xtr-TRPA1 (Fig. 11*G*) (Xla-TRPA1a, 37.8 ± 0.6 °C, $n = 34$; Xtr-TRPA1, 39.9 ± 0.5 °C, $n = 32$; data obtained from four independent preparations; *t* test, $p < 0.005$). Because Xla-TRPA1a and Xtr-TRPA1 showed similar dose dependency to cinnamaldehyde (Fig. 11*H*), heat-induced currents were normalized to the currents elicited by 0.3 mM cinnamaldehyde stimulation, as shown in Fig. 11, *A* and *C*. The results demonstrated that normalized heat-induced currents for Xla-TRPA1a were significantly larger than those for Xtr-TRPA1 (Fig. 11*I*). These observations indicated that sensitivity and activity to heat for Xla-TRPA1a was considerably higher than that for Xtr-TRPA1.

Discussion

Here we have attempted to elucidate the evolutionary changes in thermosensation between two closely related *Xenopus* species adapted to different thermal niches and have found clear species differences in heat sensitivity at both the behavioral and neurosensory levels (Fig. 1). To investigate the molecular mechanisms responsible for the species differences in heat sensation, we characterized the channel properties of TRPV1 and TRPA1, which serve as heat sensors in a wide variety of vertebrates (4–7, 10–12, 16). *X. laevis* retained duplicated paralogs for both *TRPV1* and *TRPA1*, which were likely to have been produced by the allotetraploid event that occurred in the ancestral lineage leading to *X. laevis* (Fig. 2) (27). The heat-induced activity of Xla-TRPV1a was higher than that of Xla-TRPV1b, suggesting that the former paralog may play a major role in *X. laevis* (Fig. 3*C*). Thus, we compared the heat

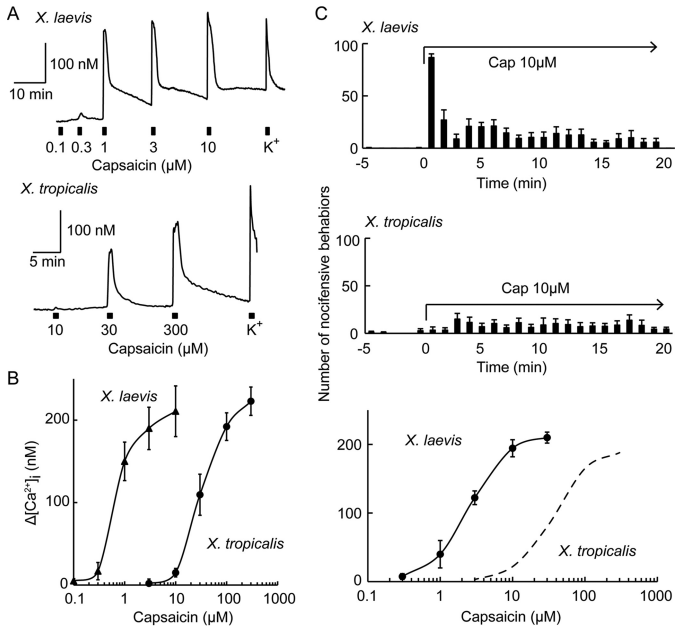

FIGURE 10. **Species differences in sensory neuron and behavioral responses to capsaicin between the two *Xenopus* species.** *A* and *B*, representative *traces* of dose-dependent changes in $[Ca^{2+}]_i$ in responses to capsaicin stimulation in DRG neurons from *X. laevis* (*A*, *upper panel*) or *X. tropicalis* (*A*, *lower panel*) and their dose dependence (*B*) ($n = 7$–16 for *X. laevis* DRG and $n = 11$–14 for *X. tropicalis* DRG). K^+, 80 mM KCl. *C*, *top* and *middle*, each *bar* represents the number of jumping behaviors in 1-min intervals before and during capsaicin (*Cap*) stimulation. *C*, *bottom*, the number of jumping behaviors in the first three 1-min intervals during capsaicin stimulation is summarized ($n = 4$ for *X. laevis* and $n = 4$ for *X. tropicalis*). Note that the data for *X. tropicalis* were adopted from Ohkita *et al.* (Ref. 4, Fig. 7*E* therein).

responses of Xla-TRPV1a with those of Xtr-TRPV1 and found that the responses to repeated heat stimulation were clearly different between the two channels (desensitization *versus* sensitization (Fig. 3, *A*, *D*, and *E*)). These observations can be interpreted as Xtr-TRPV1 being less active in response to heat stimulation compared with Xla-TRPV1a, although the sensitivity (thermal activation threshold) was similar between the two channels (Fig. 3*F*).

In the case of *X. laevis* TRPA1, both of the duplicated copies retained clear activity to heat stimulation with similar thermal activation thresholds (Fig. 11, *A* and *B*). However, the tissue distribution of Xla-TRPA1b was confined to the brain, whereas Xla-TRPA1a was widely expressed in the brain, spinal cord, and peripheral neurons, suggesting that Xla-TRPA1a plays a major role in thermosensation. The heat-evoked activity of Xla-TRPA1a was significantly higher than that of Xtr-TRPA1 (Fig. 11*I*). More importantly, the thermal activation threshold of Xla-TRPA1a was significantly lower than that of Xtr-TRPA1, which is highly consistent with the observations obtained from DRG and behavioral experiments (Figs. 1 and 11*G*). These findings strongly indicate a link between species differences in thermal sensors and behavioral responses. Recently developed genome editing technology using an artificial endonuclease will help us in addressing whether functional differences in heat sensors between the two *Xenopus* species directly alter sensory perception and behavioral responses (28–30). In summary, comparative analyses of heat sensors revealed clear functional differences between the two *Xenopus* species, which allowed us to propose the hypothesis that functional changes in heat sensors contributed to evolutionary shifts in thermosensation during adaptation to different thermal niches.

To understand the molecular basis for the evolutionary changes in heat responses of *Xenopus* TRPV1, we identified three critical amino acid substitutions by utilizing chimeric and mutagenesis experiments. We used two different strategies to identify the amino acid substitutions responsible for species differences in TRPV1. The first strategy focused on the type of amino acid substitution (substitutions occurring between amino acids with relatively different properties), and the second strategy focused on the pattern of substitutions (between Xtr-TRPV1 and Xla-TRPV1a/Xla-TRPV1b). Fortunately, we were able to identify critical mutations responsible for the species differences in *Xenopus* TRPV1 using both strategies. The single amino acid replacement of proline with leucine at position 188 (P188L) in Xtr-TRPV1 is largely responsible for the species differences in heat response. However, this mutation alone cannot explain all of the species differences, as Xtr-TRPV1 P188L did not show desensitization properties like Xla-TRPV1a (Fig. 6). In addition, the reverse mutant (Xla-TRPV1a L186P) failed to change channel properties similar to Xtr-TRPV1 (Fig. 7*B*).

In contrast, mutations at either position 156 or 232 in Xtr-TRPV1 partially increased the first heat response, and combinatory mutations at these two positions altered the mutant channel to be fully activated by the first heat stimulation (Fig. 8). Furthermore, the heat activity of Xtr-TRPV1 K156R/E232Q was similar to that of the wild type, which was in contrast to Xtr-TRPV1 P188L. Thus these two conservative substitutions at positions 156 and 232 better explain the species differences than the single, somewhat radical substitution at position 188. However, Xtr-TRPV1 K156R/E232Q again failed to show clear desensitization properties. These observations imply that additional amino acid substitutions are involved.

In the present study, we compared only two species, and thus the details of the broader evolutionary trajectory of TRPV1 channel properties have yet to be resolved. Therefore, the question remains whether the identified amino acid substitutions (at positions 156, 188, and 232 in Xtr-TRPV1) were involved directly in the functional shift in TRPV1 heat responses or were involved secondarily at a later evolutionary stage. The importance of ancestral sequence reconstruction when inferring the functional evolution and amino acid residues involved in these changes has been recognized recently (31, 32). To infer the detailed evolutionary processes of TRPV1 thermal properties in *Xenopus* lineages, multiple species comparisons are necessary. Reconstruction of the ancestral amino acid sequences and functional characterization will elucidate the detailed evolutionary processes and the molecular basis for functional changes in TRPV1 (31, 32).

What are the molecular mechanisms behind the functional differences in TRPV1 between the two *Xenopus* species? In the present study, we found contrasting thermal responses of TRPV1 to repeated heat stimulation between *X. laevis* (desensitization) and *X. tropicalis* (sensitization) (Fig. 3, *A* and *D*). *X. tropicalis* TRPV1 is the first channel to show sensitization properties to heat stimulation among all TRPV1 orthologs thus

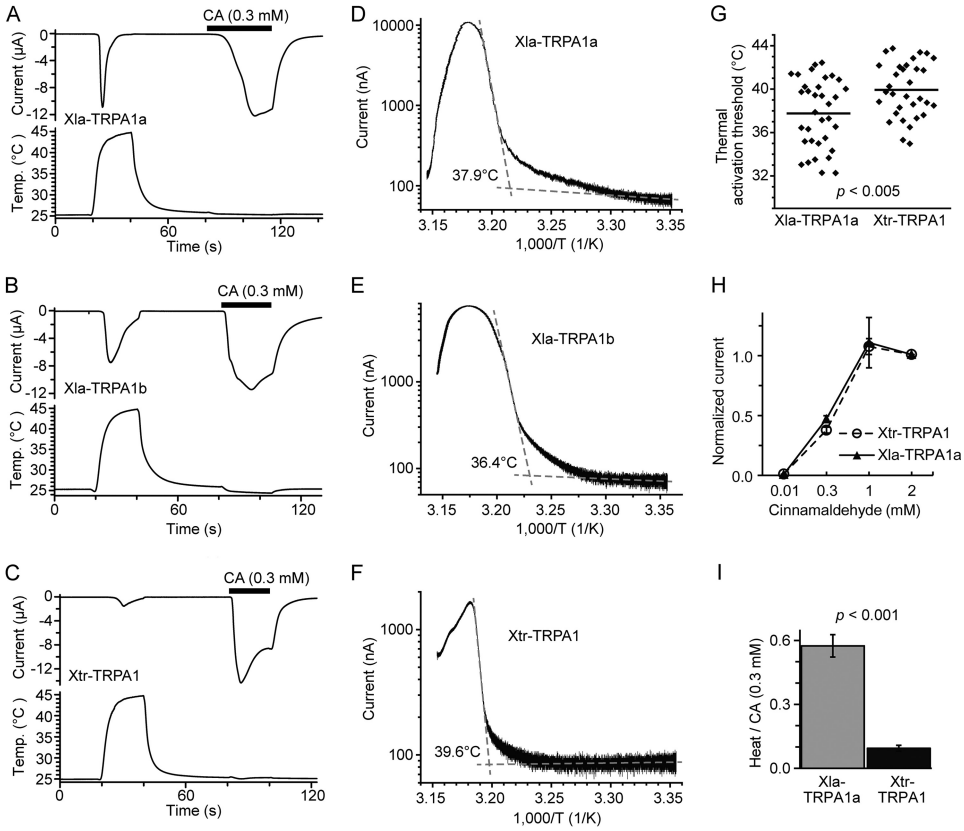

FIGURE 11. **The heat response of TRPA1 differs between the two *Xenopus* species.** *A–C*, representative *traces* for current and temperature in *Xenopus* oocytes expressing Xla-TRPA1a (*A*), Xla-TRPA1b (*B*), or Xtr-TRPA1 (*C*) in response to heat and cinnamaldehyde (*CA*) stimulation. *D–F*, representative Arrhenius plots for Xla-TRPA1a (*D*), Xla-TRPA1b (*E*), and Xtr-TRPA1 (*F*). *G*, thermal activation thresholds for Xla-TRPA1a and Xtr-TRPA1. *Dots* indicate individual values obtained from different *Xenopus* oocytes (four independent preparations) expressing Xla-TRPA1a ($n = 34$) or Xtr-TRPA1 ($n = 32$); unpaired *t* test with $p < 0.005$. *H*, dose dependence of Xla-TRPA1a or Xtr-TRPA1 in response to cinnamaldehyde (each data point consists of 4–11 observations). *I*, normalized heat-induced currents for Xla-TRPA1a and Xtr-TRPA1. Heat stimulation was applied following 0.3 mM cinnamaldehyde stimulation as shown in *A* and *C*. The current amplitude elicited by heat was normalized to that of cinnamaldehyde (Xla-TRPA1a, $n = 29$; Xtr-TRPA1, $n = 38$; four independent preparations, unpaired *t* test with $p < 0.001$).

far examined. Similar to *X. tropicalis* TRPV1, mammalian TRPV3 shows sensitization properties to repeated heat and chemical stimulation (33, 34), whereas rat TRPV1 shows clear desensitization (7). Regulatory mechanisms for TRPV channel activity have been proposed in mammals. Calmodulin has been reported to be involved in the sensitization properties of mammalian TRPV3 (35). Calmodulin is also known to be involved in capsaicin-induced desensitization in rat TRPV1 by binding to ankyrin repeat domain 3 and the C-terminal region (36–38). In the case of heat-induced desensitization of rat TRPV1, the molecular mechanisms seem to be different from capsaicin-induced desensitization, although the detailed molecular mechanisms are not well understood (39, 40). In the present study, the three amino acid substitutions responsible for the species differences in *Xenopus* TRPV1 to heat stimulation were identified in ankyrin repeat domain 1–3 (Fig. 6*A*). Thus, our findings raise the possibility that regulatory factors such as calmodulin are also involved in the species differences in *Xenopus* TRPV1 heat responses. Future biochemical and structural analyses of *Xenopus* TRPV1 will help elucidate the detailed molecular mechanisms behind the species differences in channel properties.

TRPV1 is also known as a capsaicin receptor, and its sensitivity to capsaicin is known to vary among a wide variety of vertebrate species (4–6, 16). Here we demonstrated that the sensitivity of TRPV1 to capsaicin differed widely between *X. laevis* and *X. tropicalis*, which can be explained by a single amino acid substitution occurring in the third transmembrane domain (Fig. 9). Species differences in the sensitivity to capsaicin can also be observed in DRG neurons and behavioral responses (Fig. 10), suggesting that the single amino acid substitution that occurred in the *TRPV1* genes directly alters the sensory perception and behavioral responses to capsaicin. This is the first demonstration linking the species difference in TRPV1 sensitivity to capsaicin with sensory and behavioral responses. *Xenopus* species are not likely to be exposed to capsaicin in their native environments, and thus the amino acid substitution that changed TRPV1 sensitivity to capsaicin may be a neutral one, at least within *Xenopus* lineages. However, these findings imply that a single amino acid substitution is capable of changing the functional property of a sensory receptor which, in some cases, can be related to the adaptive process during the course of evolution.

In conclusion, we have hereby identified the functional differences in the heat receptors TRPV1 and TRPA1 between two *Xenopus* species that have adapted to different thermal niches. Three amino acid substitutions are largely responsible for the species differences in the TRPV1 heat response. Our findings

will open up new opportunities to elucidate the mechanisms by which animals have evolved thermosensation when adapting to different thermal niches.

Author Contributions—S. S. and T. O. designed the study. M. O. conducted the behavioral response experiments in *Xenopus* and the calcium imaging of DRG and HeLa cells. K. T. analyzed the data from the calcium imaging experiments. S. S. and C. T. S. cloned *TRPV1* and *TRPA1* and conducted the electrophysiological experiments using *Xenopus* oocytes. S. S. and C. T. S. conducted the chimeric and mutagenesis experiments for TRPV1. S. S. reconstructed the phylogenetic trees, and C. T. S. performed the dot plot analysis. S. S., T. O., and M. T. wrote the manuscript.

Acknowledgments—We thank Dr. Yoshio Yaoita (Hiroshima University, Higashi-Hiroshima) for providing us with the Western clawed frog samples. We also thank Naomi Fukuta and Toshiyuki Sazi for valuable technical assistance.

References

1. Patapoutian, A., Peier, A. M., Story, G. M., and Viswanath, V. (2003) ThermoTRP channels and beyond: mechanisms of temperature sensation. *Nat. Rev. Neurosci.* **4,** 529–539
2. Dhaka, A., Viswanath, V., and Patapoutian, A. (2006) Trp ion channels and temperature sensation. *Annu. Rev. Neurosci.* **29,** 135–161
3. Bandell, M., Macpherson, L. J., and Patapoutian, A. (2007) From chills to chilis: mechanisms for thermosensation and chemesthesis via thermoTRPs. *Curr. Opin. Neurobiol.* **17,** 490–497
4. Ohkita, M., Saito, S., Imagawa, T., Takahashi, K., Tominaga, M., and Ohta, T. (2012) Molecular cloning and functional characterization of *Xenopus tropicalis* frog transient receptor potential vanilloid 1 reveal its functional evolution for heat, acid, and capsaicin sensitivities in terrestrial vertebrates. *J. Biol. Chem.* **287,** 2388–2397
5. Jordt, S. E., and Julius, D. (2002) Molecular basis for species-specific sensitivity to "hot" chili peppers. *Cell* **108,** 421–430
6. Gau, P., Poon, J., Ufret-Vincenty, C., Snelson, C. D., Gordon, S. E., Raible, D. W., and Dhaka, A. (2013) The zebrafish ortholog of TRPV1 is required for heat-induced locomotion. *J. Neurosci.* **33,** 5249–5260
7. Caterina, M. J., Schumacher, M. A., Tominaga, M., Rosen, T. A., Levine, J. D., and Julius, D. (1997) The capsaicin receptor: a heat-activated ion channel in the pain pathway. *Nature* **389,** 816–824
8. Myers, B. R., Sigal, Y. M., and Julius, D. (2009) Evolution of thermal response properties in a cold-activated TRP channel. *PLoS One* **4,** e5741
9. Saito, S., and Tominaga, M. (2015) Functional diversity and evolutionary dynamics of thermoTRP channels. *Cell Calcium* **57,** 214–221
10. Saito, S., Banzawa, N., Fukuta, N., Saito, C. T., Takahashi, K., Imagawa, T., Ohta, T., and Tominaga, M. (2014) Heat and noxious chemical sensor, chicken TRPA1, as a target of bird repellents and identification of its structural determinants by multispecies functional comparison. *Mol. Biol. Evol.* **31,** 708–722
11. Saito, S., Nakatsuka, K., Takahashi, K., Fukuta, N., Imagawa, T., Ohta, T., and Tominaga, M. (2012) Analysis of transient receptor potential ankyrin 1 (TRPA1) in frogs and lizards illuminates both nociceptive heat and chemical sensitivities and coexpression with TRP vanilloid 1 (TRPV1) in ancestral vertebrates. *J. Biol. Chem.* **287,** 30743–30754
12. Gracheva, E. O., Ingolia, N. T., Kelly, Y. M., Cordero-Morales, J. F., Hollopeter, G., Chesler, A. T., Sánchez, E. E., Perez, J. C., Weissman, J. S., and Julius, D. (2010) Molecular basis of infrared detection by snakes. *Nature* **464,** 1006–1011
13. Prober, D. A., Zimmerman, S., Myers, B. R., McDermott, B. M., Jr., Kim, S. H., Caron, S., Rihel, J., Solnica-Krezel, L., Julius, D., Hudspeth, A. J., and Schier, A. F. (2008) Zebrafish TRPA1 channels are required for chemosensation but not for thermosensation or mechanosensory hair cell function. *J. Neurosci.* **28,** 10102–10110
14. Chen, J., Kang, D., Xu, J., Lake, M., Hogan, J. O., Sun, C., Walter, K., Yao, B., and Kim, D. (2013) Species differences and molecular determinant of TRPA1 cold sensitivity. *Nat. Commun.* **4,** 2501
15. Saito, S., Fukuta, N., Shingai, R., and Tominaga, M. (2011) Evolution of vertebrate transient receptor potential vanilloid 3 channels: opposite temperature sensitivity between mammals and western clawed frogs. *PLoS Genet.* **7,** e1002041
16. Gavva, N. R., Klionsky, L., Qu, Y., Shi, L., Tamir, R., Edenson, S., Zhang, T. J., Viswanadhan, V. N., Toth, A., Pearce, L. V., Vanderah, T. W., Porreca, F., Blumberg, P. M., Lile, J., Sun, Y., Wild, K., Louis, J. C., and Treanor, J. J. (2004) Molecular determinants of vanilloid sensitivity in TRPV1. *J. Biol. Chem.* **279,** 20283–20295
17. Tinsley, R. C., and Kobel, H. R. (eds) (1996) *The Biology of Xenopus*, Zoological Society of London/Clarendon Press, London
18. Kashiwagi, K., Kashiwagi, A., Kurabayashi, A., Hanada, H., Nakajima, K., Okada, M., Takase, M., and Yaoita, Y. (2010) *Xenopus tropicalis*: an ideal experimental animal in amphibia. *Exp. Anim.* **59,** 395–405
19. Hirsch, N., Zimmerman, L. B., and Grainger, R. M. (2002) *Xenopus*, the next generation: *X. tropicalis* genetics and genomics. *Dev. Dyn.* **225,** 422–433
20. Hellsten, U., Harland, R. M., Gilchrist, M. J., Hendrix, D., Jurka, J., Kapitonov, V., Ovcharenko, I., Putnam, N. H., Shu, S., Taher, L., Blitz, I. L., Blumberg, B., Dichmann, D. S., Dubchak, I., Amaya, E., *et al.* (2010) The genome of the Western clawed frog *Xenopus tropicalis*. *Science* **328,** 633–636
21. Bohlen, C. J., Priel, A., Zhou, S., King, D., Siemens, J., and Julius, D. (2010) A bivalent tarantula toxin activates the capsaicin receptor, TRPV1, by targeting the outer pore domain. *Cell* **141,** 834–845
22. Tamura, K., Stecher, G., Peterson, D., Filipski, A., and Kumar, S. (2013) MEGA6: Molecular Evolutionary Genetics Analysis, version 6.0. *Mol. Biol. Evol.* **30,** 2725–2729
23. Jones, D. T., Taylor, W. R., and Thornton, J. M. (1992) The rapid generation of mutation data matrices from protein sequences. *Comput. Appl. Biosci.* **8,** 275–282
24. Saitou, N., and Nei, M. (1987) The neighbor-joining method: a new method for reconstructing phylogenetic trees. *Mol. Biol. Evol.* **4,** 406–425
25. Felsenstein, J. (1985) Confidence limits on phylogenies: an approach using the bootstrap. *Evolution* **39,** 783–791
26. Schwartz, S., Zhang, Z., Frazer, K. A., Smit, A., Riemer, C., Bouck, J., Gibbs, R., Hardison, R., and Miller, W. (2000) PipMaker: a Web server for aligning two genomic DNA sequences. *Genome Res.* **10,** 577–586
27. Evans, B. J., Kelley, D. B., Tinsley, R. C., Melnick, D. J., and Cannatella, D. C. (2004) A mitochondrial DNA phylogeny of African clawed frogs: phylogeography and implications for polyploid evolution. *Mol. Phylogenet. Evol.* **33,** 197–213
28. Guo, X., Zhang, T., Hu, Z., Zhang, Y., Shi, Z., Wang, Q., Cui, Y., Wang, F., Zhao, H., and Chen, Y. (2014) Efficient RNA/Cas9-mediated genome editing in *Xenopus tropicalis*. *Development* **141,** 707–714
29. Blitz, I. L., Biesinger, J., Xie, X., and Cho, K. W. (2013) Biallelic genome modification in F(0) *Xenopus tropicalis* embryos using the CRISPR/Cas system. *Genesis* **51,** 827–834
30. Nakayama, T., Fish, M. B., Fisher, M., Oomen-Hajagos, J., Thomsen, G. H., and Grainger, R. M. (2013) Simple and efficient CRISPR/Cas9-mediated targeted mutagenesis in *Xenopus tropicalis*. *Genesis* **51,** 835–843
31. Yokoyama, S. (2013) Synthetic biology of phenotypic adaptation in vertebrates: the next frontier. *Mol. Biol. Evol.* **30,** 1495–1499
32. Dean, A. M., and Thornton, J. W. (2007) Mechanistic approaches to the study of evolution: the functional synthesis. *Nat. Rev. Genet.* **8,** 675–688
33. Peier, A. M., Reeve, A. J., Andersson, D. A., Moqrich, A., Earley, T. J., Hergarden, A. C., Story, G. M., Colley, S., Hogenesch, J. B., McIntyre, P., Bevan, S., and Patapoutian, A. (2002) A heat-sensitive TRP channel expressed in keratinocytes. *Science* **296,** 2046–2049
34. Xu, H., Ramsey, I. S., Kotecha, S. A., Moran, M. M., Chong, J. A., Lawson, D., Ge, P., Lilly, J., Silos-Santiago, I., Xie, Y., DiStefano, P. S., Curtis, R., and Clapham, D. E. (2002) TRPV3 is a calcium-permeable temperature-sensitive cation channel. *Nature* **418,** 181–186
35. Xiao, R., Tang, J., Wang, C., Colton, C. K., Tian, J., and Zhu, M. X. (2008) Calcium plays a central role in the sensitization of TRPV3 channel to repetitive stimulations. *J. Biol. Chem.* **283,** 6162–6174

36. Rosenbaum, T., Gordon-Shaag, A., Munari, M., and Gordon, S. E. (2004) Ca2+/calmodulin modulates TRPV1 activation by capsaicin. *J. Gen. Physiol.* **123,** 53–62
37. Numazaki, M., Tominaga, T., Takeuchi, K., Murayama, N., Toyooka, H., and Tominaga, M. (2003) Structural determinant of TRPV1 desensitization interacts with calmodulin. *Proc. Natl. Acad. Sci. U.S.A.* **100,** 8002–8006
38. Lishko, P. V., Procko, E., Jin, X., Phelps, C. B., and Gaudet, R. (2007) The ankyrin repeats of TRPV1 bind multiple ligands and modulate channel sensitivity. *Neuron* **54,** 905–918
39. Joseph, J., Wang, S., Lee, J., Ro, J. Y., and Chung, M. K. (2013) Carboxyl-terminal domain of transient receptor potential vanilloid 1 contains distinct segments differentially involved in capsaicin- and heat-induced desensitization. *J. Biol. Chem.* **288,** 35690–35702
40. Tominaga, M., Caterina, M. J., Malmberg, A. B., Rosen, T. A., Gilbert, H., Skinner, K., Raumann, B. E., Basbaum, A. I., and Julius, D. (1998) The cloned capsaicin receptor integrates multiple pain-producing stimuli. *Neuron* **21,** 531–543